Ocean & Sea Ice SAF

Global Sea Ice Concentration Climate Data Records

Product User's Manual

Document version: 3.1
Data set version: 3.0

OSI-450-a: 10.15770/EUM_SAF_OSI_0013
OSI-430-a: 10.15770/EUM_SAF_OSI_0014
OSI-458: 10.15770/EUM_SAF_OSI_0015

April 2023

Atle M Sørensen, Thomas Lavergne, and Steinar Eastwood
MET Norway

The EUMETSAT Network of Satellite Application Facilities

OSI SAF
Ocean and Sea Ice

Documentation Change Record

Document version	Data set version	Date	Change Description
v1.0 draft	v2.0	17.02.2017	First version of PUM for OSI-450
v1.0	v2.0	22.03.2017	Updated after review
v2.0	v2.0	04.03.2019	Updated to include OSI-430-b and updated with comments from ORR.
v2.1	v2.0	18.02.2021	New section 2 “Dates with artifacts”. Section 6: add recent literature in discussing the known limitations of the product.
v3.0_draft	v3.0	17.06.2022	Updated PUM for the “v3” CDRs: OSI-450-a, OSI-430-a, OSI-458 (draft version before DRR/ORR).
v3.0	v3.0	24.08.2022	Revise PUM for the “v3” CDRs: OSI-450-a, OSI-430-a, OSI-458 (version after DRR/ORR).
v3.1	v3.0	17.04.2023	Improve the documentation of the monthly product files (add table of missing months). Add python code example to reconstruct the full SIC field from ice_conc, raw_ice_conc_values, and status_flag. Remove URL to ftp servers, mention FileZilla as an alternative tool.

CONTENTS

1. Introduction

1.1 The EUMETSAT Ocean and Sea Ice SAF

The Satellite Application Facilities (SAFs) are dedicated centres of excellence for processing satellite data – hosted by a National Meteorological Service – which utilise specialist expertise from institutes based in Member States. EUMETSAT created Satellite Application Facilities (SAFs) to complement its Central Facilities capability in Darmstadt. The Ocean and Sea Ice Satellite Application Facility (OSI SAF) is one of eight EUMETSAT SAFs, which provide users with operational data and software products. More on SAFs can be read at www.eumetsat.int.

OSI SAF produces (on an operational basis) a range of air-sea interface products, namely: wind, sea ice characteristics, Sea Surface Temperatures (SST), Surface Solar Irradiance (SSI) and Downward Longwave Irradiance (DLI). The sea ice products include sea ice concentration, the sea ice emissivity at 50 GHz, sea ice edge, sea ice type and sea ice drift and sea ice surface temperature (from mid 2014).

The OSI SAF consortium is hosted by Météo-France. The sea ice processing is performed at the High Latitude processing facility (HL centre), operated jointly by the Norwegian and Danish Meteorological Institutes.

Note: The ownership and copyrights of the data set belong to EUMETSAT. The data is distributed freely, but EUMETSAT must be acknowledged when using the data. EUMETSAT's copyright credit must be shown by displaying the words "copyright (year) EUMETSAT" on each of the products used. We welcome anyone to use the data. The comments that we get from our users is an important input when defining development activities and updates, and user feedback to the OSI SAF project team is highly valued.

1.2 Disclaimer

Acknowledgement and citation

Use of the product(s) should be acknowledged with the following citations:

EUMETSAT Ocean and Sea Ice Satellite Application Facility, Global sea ice concentration climate data record 1978-2020 (v3.0, 2022), OSI-450-a, doi: 10.15770/EUM_SAF_OSI_0013, data (for [extracted period], [extracted domain],) extracted on [download date]

EUMETSAT Ocean and Sea Ice Satellite Application Facility, Global sea ice concentration interim climate data record (v3.0, 2022), OSI-430-a, doi: 10.15770/EUM_SAF_OSI_0014, data (for [extracted period], [extracted domain],) extracted on [download date]

EUMETSAT Ocean and Sea Ice Satellite Application Facility, Global medium resolution sea ice concentration climate data record 2002-2020 (v3.0, 2022), OSI-458, doi: 10.15770/EUM_SAF_OSI_0015, data (for [extracted period], [extracted domain],) extracted on [download date]

1.3 Scope

This report is the Product User's Manual (PUM) for three OSI SAF Sea Ice Concentration Climate Data Records (OSI-450-a, OSI-430-a, OSI-458 see next section for definition).

The PUM gives a high-level overview of the input data used and the processing steps involved, but is more importantly a reference for how the product files are formatted and named. Geographical and temporal coverage are described, in addition to known limitations of these data records.

1.4 Overview

OSI-450-a, OSI-430-a and OSI-458 constitute the *third major release* of the OSI SAF Global Sea Ice Concentration Climate Data Records. In short, these three CDRs can be summarized as:

- OSI-450-a : The Global Sea Ice Concentration Climate Data Record, based on coarse resolution imagery from SMMR, SSM/I, and SSMIS and covering 1978-2020.
- OSI-430-a : The Global Interim CDR (ICDR) based on coarse resolution imagery from SSMIS and providing an extension of OSI-450-a starting january 2021.
- OSI-458 : The Global Sea Ice Concentration Climate Data Record based on medium resolution imagery from AMSR-E (2002-2011) and AMSR2 (2012-2020). OSI-458 is a Research to Operations transfer from ESA CCI.

OSI-450-a is a fixed-length climate data record (1978-2020) based on re-calibrated satellite data and the state-of-the-art ERA5 reanalysis. OSI-458 is also a fixed-length climate data record (2002 – 2020 with a data gap in 2011-2012) that achieves better spatial resolution than OSI-450-a by using the AMSR-E and AMSR2 satellites. OSI-430-a provides a timely extension of OSI-450-a starting in January 2021. OSI-430-a has two data streams: 1) the "nominal" ICDR that applies exactly the same algorithm as OSI-450-a and has a latency of 16 days, and 2) the "fast-track" ICDR that applies a slightly different algorithm (tie-point selection) and achieves a latency of 2 days. The fast-track ICDR was introduced for the third release after requests from operational climate users.

The *first major version* of the OSI SAF sea-ice concentration CDRs was called OSI-409 and was initiated in 2006 (Tonboe et al., 2016).

The *second major version* was OSI-450, complemented by the ICDR OSI-430-b (Lavergne et al., 2019). Some of the algorithms implemented in OSI-450 and OSI-430-b were contributed to by the ESA CCI Phase 1 and 2 projects. ESA CCI also released their own SIC CDR at medium resolution (based on AMSR-E and AMSR2 data), notably the SICCI-25km dataset.

For this *third major version*, new R&D contributions from ESA CCI (now CCI+) are acknowledged. On the one hand, new R&D contributions from ESA CCI contribute to the v3 SIC algorithms used in the OSI SAF CDR. In addition, OSI-458 is a newer and better version of SICCI-25km that was developed in the ESA CCI Phase 2 project (Research to Operation transfer from ESA CCI to EUMETSAT OSI SAF).

It is noteworthy that ESA CCI+ is also producing their own SIC datasets, that are complementary to those of the OSI SAF (see climate.esa.int/seaice for updates). The datasets from CCI+ Sea Ice will target higher spatial resolution than those of the OSI SAF, at the cost of being shorter time series. The pros and cons of the sea-ice concentration datasets from OSI SAF and CCI+ are described in the Product User Manuals of both projects.

Figure 1: The ESA Climate Change Initiative Sea Ice project contributed to the OSI SAF climate data records through a number of algorithm developments.

1.5 Glossary

Acronym	Description
AMSR	Advanced Microwave Scanning Radiometer
ATBD	Algorithm Theoretical Basis Document
CCI	Climate Change Initiative
CDOP	Continuous Developments and Operations Phase
CDR	Climate Data Record
CLASS	NOAA's Comprehensive Large Array-data Stewardship System
DMI	Danish Meteorological Institute
DMSP	Defence Meteorological Satellite Program
ECMWF	European Centre for Medium range Weather Forecast
ESA	European Space Agency
EUMETSAT	European Organization for the Exploitation of Meteorological Satellites
FCDR	Fundamental Climate Data Record
FoV	Field Of View
FYI	First Year Ice
GR	Gradient Ratio
ICDR	Interim Climate Data Record
MET Norway	Norwegian Meteorological Institute
NASA	National Aeronautics and Space Administration
NOAA	National Oceanographic and Atmospheric Administration
NH	Northern Hemisphere
NSIDC	National Snow and Ice Data Center
NWP	Numerical Weather Prediction
OSI SAF	Ocean and Sea Ice Satellite Application Facility
OWF	Open Water Filter

PCR	Product Consolidation Review
RTM	Radiative Transfer Model
SAR	Synthetic Aperture Radar
SH	Southern Hemisphere
SIC	Sea Ice Concentration
SICCI	ESA CCI Sea Ice project
SMMR	Scanning Multichannel Microwave Radiometer
SSM/I	Special Sensor Microwave/Imager
SSMIS	Special Sensor Microwave Imager Sounder
Tb	Brightness Temperature
TBC	To Be Confirmed
TBD	To Be Determined
TBW	To Be Written
WF	Weather Filter

1.6 Reference and Applicable documents

Detailed information on the algorithm and the processing of the products are to be found in the Algorithm Theoretical Basis Document (ATBD) [RD-1]. Results from the validation exercise are gathered in an associated Scientific Validation Report (SVR) [RD-2]

1.6.1 Reference documents

[RD-1] EUMETSAT OSI SAF Algorithm Theoretical Baseline Document for the Global Sea Ice Concentration Climate Data Records v3 (OSI-450-a, OSI-430-a, OSI-458), SAF/OSI/CDOP3/DMI_Met/SCI/MA/270, version v3.0, August 2022

[RD-2] EUMETSAT OSI SAF Validation Report for the Global Sea Ice Concentration Climate Data Records v3 (OSI-450-a, OSI-430-a, OSI-458), SAF/OSI/CDOP3/DMI/SCI/RP/285, version v3.0, August 2022

1.6.2 Applicable documents

[AD-3] EUMETSAT OSI SAF Product Requirements Document, SAF/OSI/CDOP3/MF/MGT/PL/2-001, version 1.90, 31/12/2021

2. Dates with artifacts

Despite our careful examination before the release of OSI-450-a, OSI-430-a, and OSI-458, there might still be artefacts in some of the product files. We encourage our users to contact us if they find such artefacts, so that they can be documented here.

We mention here the thorough visual inspection conducted by Stefan Kern from the Integrated Climate Data Center at University of Hamburg. He documents a number of dates with potential artefacts at an ICDC webpage dedicated to the OSI-450-a and OSI-430-a data (under Data quality).

Readers are also refered to section 6. for a more general description of known limitations with the product.

3. Input data

This chapter describes the SMMR, SSM/I, SSMIS AMSR-E and AMSR2 satellite data, as well as numerical weather prediction (NWP) data, used for this third version. Figure 2 shows a timeline of the satellite missions having relevant passive microwave sensors, many of which enter our SIC CDRs.

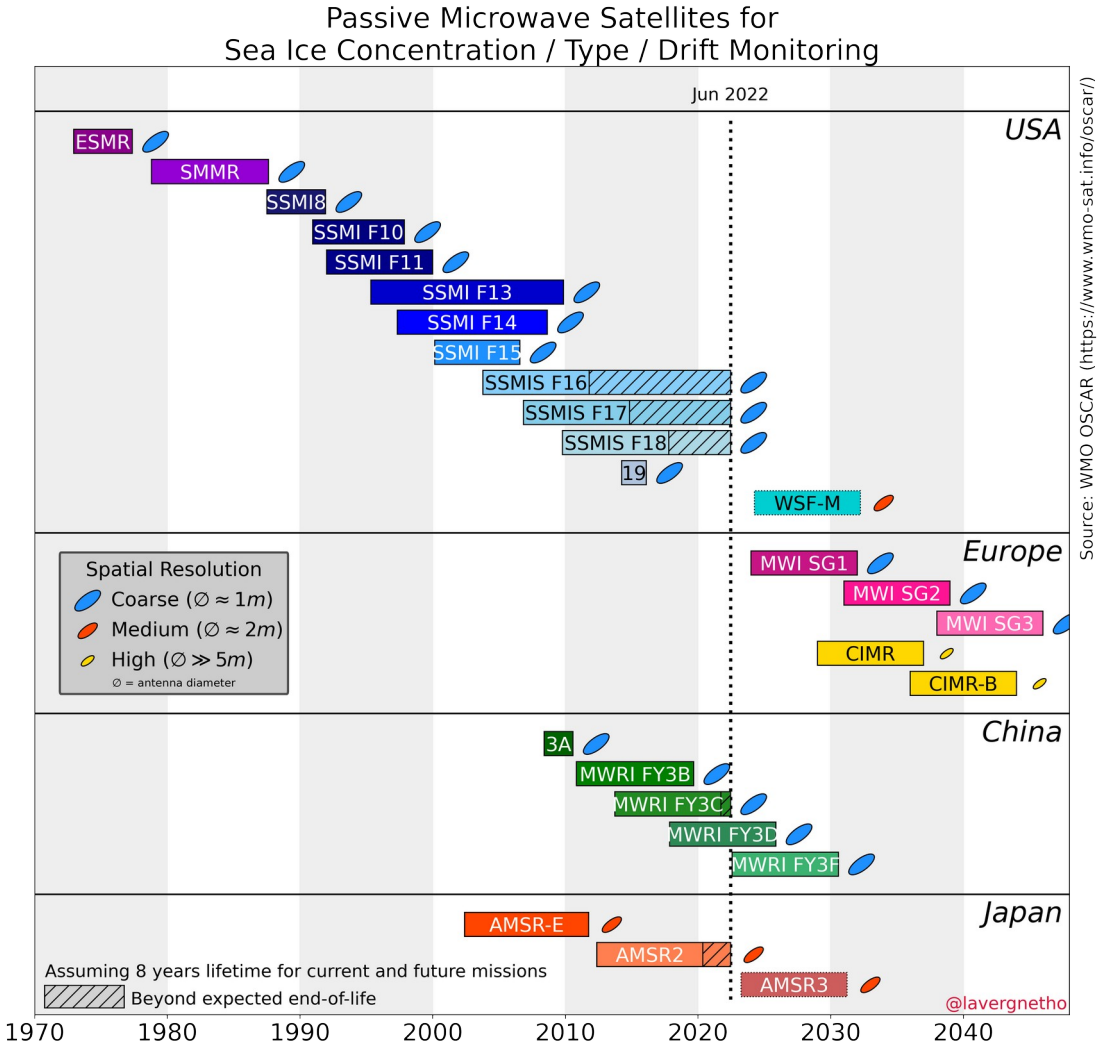

Figure 2: Timeline of the Passive Microwave satellite missions relevant for sea-ice concentration/extent/area monitoring (as well as Type and Drfit) with an indication of their spatial resolution capabilities. OSI-450-a and OSI-430-a use SMMR, all SSM/I, and SSMIS. OSI-458 uses AMSR-E and AMSR2. The horizontal bars represent satellite missions, which are colored by sensor family.

3.1 The SMMR data

The Scanning Multichannel Microwave Radiometer (SMMR) instrument on board the Nimbus 7 satellite operated from October 1978 to 20th August 1987 (Gloersen et al., 1992). For most of the period, the instrument was operated only every second day, due to power supply limitations. The instrument had 10 channels, from six Dicke radiometers, at five frequencies (6.6, 10.7, 18.0, 21.0, 37.0 GHz) and vertical and horizontal polarization (Table 1). The scanning across track was ensured by tilting the reflector from side to side while maintaining

constant incidence angle on the ground of about 50.2°. The scan track on the ground formed a 780 km wide arc in front of the satellite (Gloersen and Barath, 1977). Because of the satellite orbit inclination and swath width there is no coverage poleward of 84°.

Frequency (GHz)	Polarizations	Sampling (average)	Field of view	
			Along-track	Cross-track
6.6	H,V	25 km	148 km	95 km
10.7	H,V	25 km	91 km	59 km
18.0	H,V	25 km	55 km	41 km
21.0	H,V	25 km	46 km	30 km
37.0	H,V	25 km	27 km	18 km

Table 1: Characteristics of the Nimbus 7 SMMR channels (Gloersen and Barath, 1977).

Readers interested in the processing, calibration and quality check steps applied in the FCDR will find many more details in the CM-SAF documentation and Fennig et al. (2020).

3.2 The SSM/I data

The Special Sensor Microwave/Imager (SSM/I) sensors on board the Defence Meteorological Satellite Program (DMSP) satellites started its record with the F08 satellite on 9th July 1987, shortly before the SMMR ceased to operate. The SSM/I is a total power radiometer, with a conical scan measuring the upwelling radiation from the Earth at a constant incidence angle of about 53.1° at four frequencies (19.3, 22.2, 37.0, 85.5 GHz). The swath width is about 1400 km and the polar observation hole extends to 87°.

The SSM/I data set used for this reprocessing was prepared by EUMETSAT CM SAF and covers the period of available DMSP satellite instruments from 1987 to 2008 (F08, F10, F11, F13, F14, F15) (see Table 2). Some SSM/I instruments continued their mission further than 2008, but these data are not included in the CM SAF FCDR.

The SSM/I instruments have five low-frequency channels that are mostly similar to some of those on SMMR. In addition, two higher-frequency channels at 85GHz, with twice the sampling rate and better spatial resolution, are available on the SSM/I starting with DMSP F10 (the 85 GHz channels had a malfunction on F08). Characteristics of the SSM/I channels are listed in Table 3.

Satellite	Period covered
F08	Jul 1987 – Dec 1991
F10	Jan 1991 - Nov 1997
F11	Jan 1992 – Dec 1999
F13	May 1995 – Dec 2008
F14	May 1997 – Aug 2008
F15	Feb 2000 – Jul 2006

Table 2: The different satellite missions carrying the SSM/I instrument and the periods they cover.

Frequency (GHz)	Polarizations	Sampling	Footprint size	
			Along-track	Cross-track
19.35	H,V	25 km	69 km	43 km
22.235	V	25 km	50 km	40 km
37.0	H,V	25 km	37 km	28 km
85.5	H,V	12.5 km	15 km	13 km

Table 3: Characteristics of the different SSM/I channels (from Wentz, 1991).

Readers interested in the processing, calibration and quality check steps applied in the FCDR will find many more details in the CM-SAF documentation and Fennig et al. (2020).

3.3 The SSMIS data

The SSMIS instruments are a slight evolution of the SSM/I concept, and most characteristics that drive the design of SIC CDRs are similar to SSM/I. Noticeable differences are the size of the polar observation hole (89°), and the center frequency of the high-frequency channels (91.1 GHz). The SSMIS instruments were also on board DMSP satellites, and we use F16, F17, and F18 missions (F19 was a short-lived mission, and F20 was never launched). DMSP F18 is thus the last available SSMIS instrument.

Data from three DMSP platforms are used in the CDR OSI-450-a: F16 (Nov 2005 - Dec 2013), F17 (Dec 2006 - Dec 2020), and F18 (Mar 2010 - Dec 2020). They are from CM SAF FCDR.

In addition, SSMIS F16, F17, and F18 are processed to extend the ICDR OSI-430-a from January 2021 onwards. This operational data stream is from NOAA CLASS, NOAA's data center for environmental data (https://www.avl.class.noaa.gov/saa/products/welcome).

3.4 The AMSR-E data

The AMSR-E instrument on board the Earth Observing System (EOS) satellite Aqua recorded passive microwave data from 1st June 2002 until 4th October 2011. This instrument measured vertically and horizontally polarized brightness temperatures at 7 frequencies (6.9, 7.2, 10.7, 18.7, 23.8, 36.5 and 89 GHz), thus 14 channels in all. Thanks to a larger antenna reflector, AMSR-E had significantly better spatial resolution than SSM/I or SSMIS. It also had a wider swath, and thus a smaller polar observation hole (89.5°).

OSI-458 uses AMSR-E data (June 2002 to October 2011) from NSIDC FCDR AE_L2A V003 by Ashcroft and Wentz (2013).

3.5 The AMSR2 data

The AMSR2 instrument on board the Global Change Observation Mission – Water (GCOM-W1) satellite provides similar data to the AMSR-E instrument (no 7.2 GHz channels), with slightly better resolution.

OSI-458 uses AMSR2 data (July 2012 to December 2020) from JAXA's archive of L1R data stream.

3.6 Numerical Weather Prediction data

The microwave radiation emitted by the ocean and sea ice travels through the Earth's atmosphere before being recorded by the satellite sensors. Scattering, reflection, and

emission in the atmosphere add or subtract contributions to the radiated signal, and challenge our ability to accurately quantify sea-ice concentration.

A central step in our Level-2 processing is thus the explicit correction of the Tb for the atmospheric contribution to the top of the atmosphere radiation. For this purpose, we use global hourly fields from the C3S ERA5 reanalysis (produced by ECMWF, see Hersbach et al., 2020). Fields of 10m wind speed, 2m air temperature, total column water vapour and total column cloud liquid water are used.

The ERA5 reanalysis was recently extended to start in 1950, and is thus available throughout the time period of the CDRs OSI-450-a and OSI-458. The skill of ERA5 changes in Jan 1979 due to modifications in (1) the observing system, (2) the ocean boundary conditions (SIC data), and (3) the data assimilation system (background error covariances). However, our investigations and validation results do not reveal a notable impact on the Oct-Dec 1978 SICs.

For the main stream of OSI-430-a, we use ERA5T data. ERA5T are initial release data, i.e. data no more than three months behind real time, made available with 5 days latency.

The fast-track stream of OSI-430-a uses the operational NWP analysis and forecast from ECMWF.

3.7 Binary land mask

Land masks for the target 25×25 km grids (one for NH and one for SH) are prepared from two higher resolution sources. The ocean mask is from the ESA SST CCI OSTIA L4 product (version 2.1), at 0.05×0.05° resolution (~6x3 km in the polar regions). The lake mask is from the ESA Lakes CCI (ESACCI-LAKES_mask_v1.nc) at 0.0083×0.0083° (~1x0.5 km in the polar regions). The OSTIA L4 land mask is selected because of the long tradition of preparing SST+SIC analyses. We have also investigated other land masks (such as that of the ESA CCI Land Cover project, but it did not make a difference at these spatial scales.

These high-resolution binary masks are first regridded to the EASE2 25×25 km NH and SH grids to prepare “density_of_land”, “density_of_ocean”, and “density_of_lakes” variables (all 3 in [0,1] and the sum equals 1). The Caspian Sea, which is water body both in the SST and lakes mask, is considered a lake for our Sea Ice CDRs.

Then, a binary “smask” (surface mask) variable is prepared from the three density_of_* fields. Variable “smask” takes on values "0: ocean, 1: ocean coastline, 2: land, 4: lake coastline, 5: lake" (see Figure 3). In the final product, sea-ice concentration values are provided for all grid cells with smask 0 (ocean) and 5 (lakes).

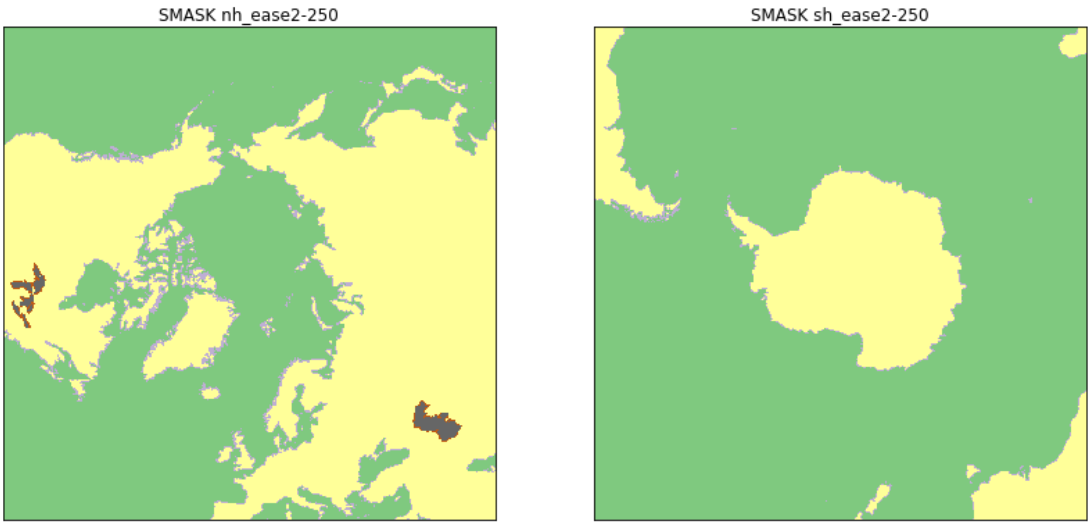

Figure 3: Variable "smask" used in the SIC CDRs on the EASE2 25.0 km grids (left: NH, right: SH). Ocean (smask=0): green, Ocean coastline (smask=1): light grey, Land (smask=2): yellow, Lake coastline (smask=4): red, Lake (smask=5): dark grey.

The binary smask is tuned to closely match that of the NSIDC SIC CDR (the NSIDC "SSM/I" 25 km Polar Stereographic mask) in the regions they have in common. On average, this corresponds to setting all 25×25 km grid cells with a fraction of land lower than 30 % to water (ocean or lake). There is no right or wrong binary land mask at such coarse resolution, and the decision to tune to the NSIDC SIC CDR land mask is to help an intercomparison of data records.

For the new "v3" CDRs, it was decided to only keep the largest lake systems (Caspian Sea and the US Great Lakes) and not consider smaller inland water (e.g. Great Bear Lake, Baikal, Ladoga). Experience from "v2" datasets indicates that our CDRs had limited value over smaller lakes due to the coarse resolution of the sensors.

3.8 Sea Ice Extent Climatology

We use a monthly varying maximum sea-ice extent climatology to filter out grossly erroneous sea-ice detection far from the polar regions, and along the coastlines at mid to high latitudes. A monthly varying climatology is required because of the large seasonal variability of the polar sea ice extent.

The monthly varying maximum sea-ice extent climatology implemented in the NSIDC SIC CDR v3 (Peng et al. 2013 , Meier et al., 2017) was used as a basis for our climatology. The NSIDC climatology is described in their Climate-ATBD (available from the dataset landing page of Meier et al., 2017) and covers the years up-until 2007.

We then did some modifications to the climatologies, mainly manual editing of some single pixels, based on US National Ice Center, Canadian Ice Service, and Norwegian and Finnish Ice Service ice charts (e.g. along the coast of northern Norway, for some summer months in the vicinity of Nova Scotia and in the Baltic Sea and Gulf of Finland). The climatology of peripheral seas and large freshwater bodies (e.g. Bohai and Northern Yellow Seas, Great Lakes, Caspian Sea, and Sea of Azov) was also revisited.

Compared to “v2”, the main change in the “v3” climatology is a focus on the coastal regions during summer, especially the Baltic Sea. These coastal regions are very challenging for our coarse resolution CDRs OSI-450-a and OSI-430-a (to a lesser extent OSI-458) because of land spill-over. In the preparation phase for “v3”, we liased with the Finnish Ice Service and adapted the regional climatology using their input.

The cleaned climatologies are then expanded with a buffer zone of 150 km in the NH and 250 km in the SH. This expansion is not applied in the Baltic Sea during summer months. The larger expansion in SH is to cope with the slight positive trends in the SH sea-ice extent (Parkinson, 2019). Finally, the “v2” SIC CDR and ICDR (covering 1979-2020) was used to check that the new climatology does not cut away true sea-ice.

3.9 Beyond SSMIS

OSI-430-a relies on SSMIS for the daily extension of the data record. However, the three SSMIS are aging, and long past their design lifetime. SSMIS F19 failed early, and F20 was decomissioned before launch. The AMSR2 is also aging and is too dissimilar to SSMIS to ensure climate consistency at a daily SIC level. There is thus a non-zero risk that the SSMIS extensions of OSI-430-a would stop before the EPS-SG MicroWave Imager (MWI) is operational and processed in our chains (launch date currently 2023).

At the OSI SAF, a contigency plan has been to look into the processing of China’s MicroWave Radiometer Imager (MWRI) on board the Feng-Yun 3 satellites. Preliminary results are encouraging (FY3D). The chains will be finalized and brought to operation in the event when additional SSMIS fail before EPS-SG MWI is ready. This contigency plan is not only for OSI-430-a, but for several other sea-ice products.

4. Processing scheme

Figure 4 gives an overview of the processing chain used for the SIC CDRs. The red boxes are data (stored in data files) and the blue boxes are processing elements that apply algorithms to the data. The whole process is structured into four chains, at Level 1P (left), Level 2, Level 3, and Level 4 (right). The input Level 1 (L1) data files hold the fields observed by the satellite sensors at the top of the atmosphere, in satellite projection: the brightness temperatures (Tb) are structured in swath files. The Level 1 Preprocessing (L1P) prepares the L1B swath files for SIC processing. The Level 2 (L2) chain transforms these into the geophysical variables of interest, but still on swath projection: the SIC, its associated uncertainties, and flags. The L2 chain holds an iteration (marked by the “2nd iteration” grey box) similar to the workflow in Tonboe et al. (2016) and stemming from the developments of Andersen et al. (2007). This iteration implements two key correction schemes: the atmospheric correction algorithm at low-concentration range and a correction for systematic errors at high-concentration range. The Level 3 (L3) chain collects the L2 data files and produces daily composited fields of SIC, uncertainties, and flags on regularly spaced polar grids. These fields can and will typically exhibit data gaps, e.g. in case of missing satellite data. The Level 4 (L4) chain fills the gaps, applies extra corrections, and formats the data files that will appear in the CDR. The Algorithm Theoretical Basis Document (ATBD) [RD-2] contains all the details of the algorithms and processing steps involved.

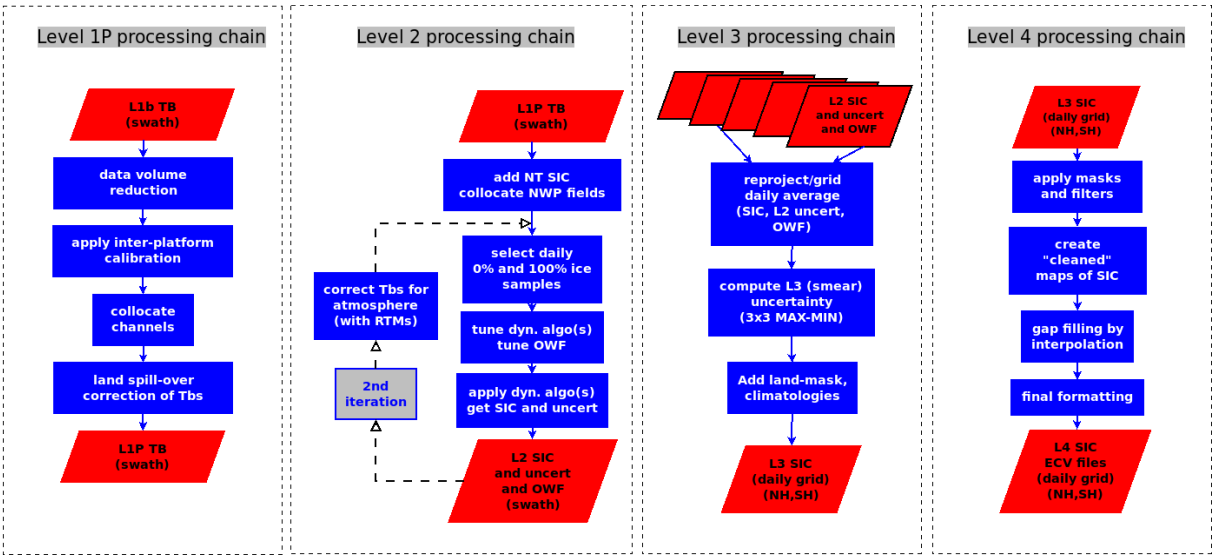

Figure 4: From left to right, the four main elements (Level 1P, Level 2, Level 3, and Level 4) in the sea-ice concentration (SIC) processing workflow. The red boxes depict data files, the blue boxes correspond to individual steps (a.k.a. algorithms) in the processing. The files that exit a processing chain (e.g. the “L2 SIC and uncert and OWF” at the bottom of the Level 2 processing chain) are the input for the next level of processing. Acronyms: NT is the Nasa Team algorithm, OWF is open-water filter, RTM is radiative transfer model, uncert stands for uncertainty.

5. Product description

This chapter gives a description of the product specification, meta data, data format and product availability.

5.1 Product specification

The product files contain six variables (in addition to latitude, longitude, time, and other CF-related information):

- main (filtered) sea ice concentration (`ice_conc`)
- raw sea ice concentration values (`raw_ice_conc_values`)
- total uncertainty (`total_standard_uncertainty`)
- smearing uncertainty (`smearing_standard_uncertainty`)
- algorithm uncertainty (`algorithm_standard_uncertainty`)
- status flag (`status_flag`)

The definitions of these fields are given in the sections below. These fields are all covering the same grid.

For our v2 users, the only difference in variable names is that the three uncertainty variables are now named "_uncertainty" while they were (erroneously) named "_error" in v2.

5.1.1 Sea ice concentration (ice_conc)

Sea ice concentration is the ocean area fraction of a cell covered by sea ice. It is given as a real number in percentage, with a range from 0-100%. This variable holds sea ice concentration maps after several filters (e.g. the open water filter) and post-processing steps (e.g. interpolation and thresholding) have been applied. It is the main variable for users of this Climate Data Record.

Examples are shown in Figure 5 and Figure 6. Figure 6 illustrates the greater level of details available fom OSI-458 thanks to the use of the AMSR missions (in place of SSM/I and SSMIS). OSI-458 is on the same EASE2 25 km grid as OSI-450-a but the true spatial resolution of OSI-450-a is somewhat coarser than 25 km.

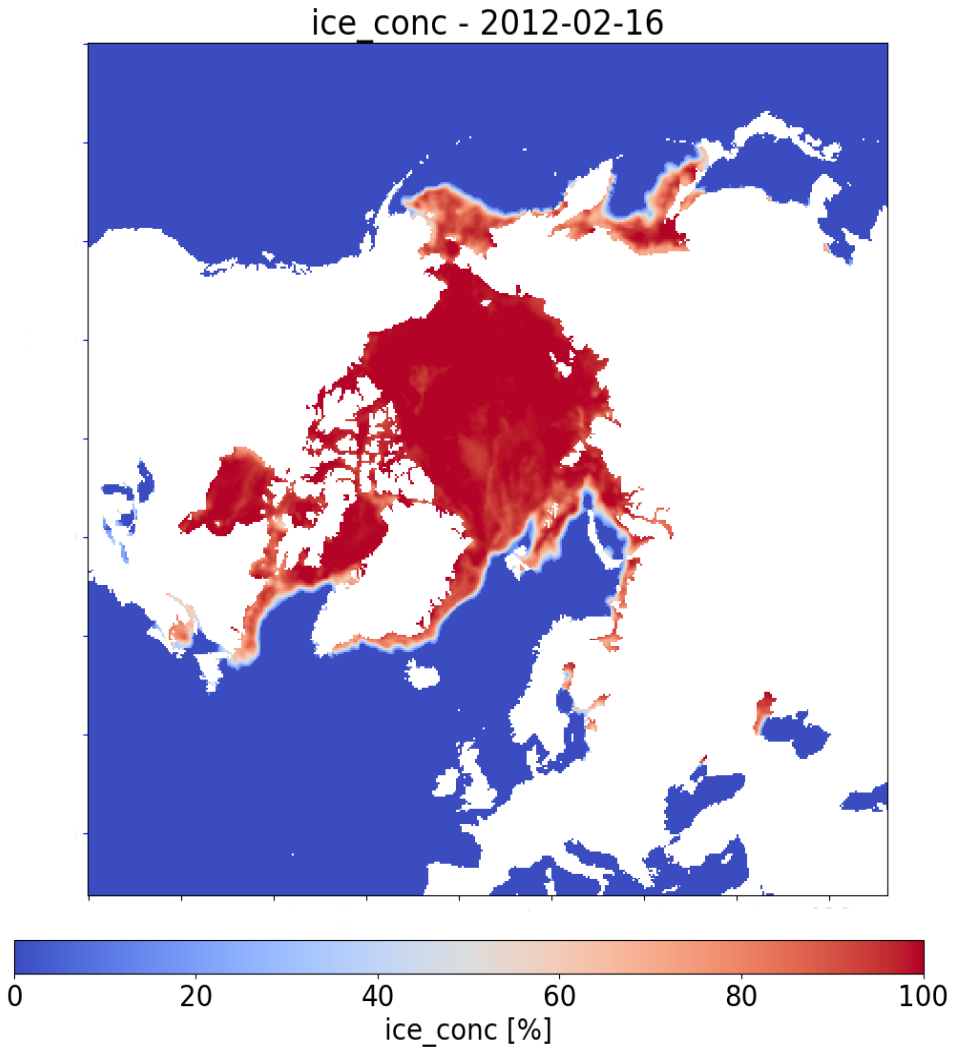

Figure 5: OSI-450-a sea ice concentration (ice_conc) on 16th February 2012

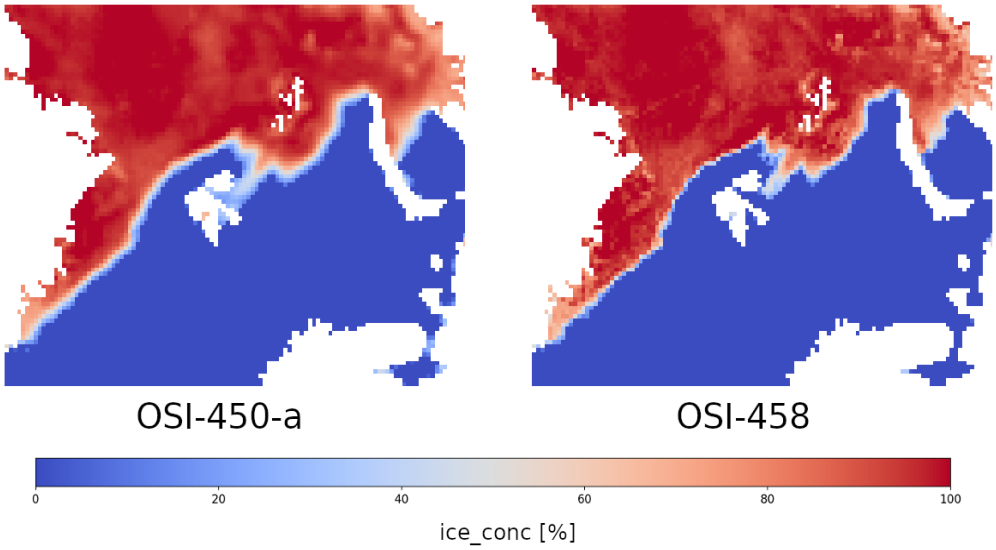

Figure 6: OSI-450-a (left) and OSI-458 (right) sea ice concentrations on 28th October 2004

5.1.2 Raw sea ice concentration values

Variable `raw_ice_conc_values` contains the original ("raw") values of the sea ice concentration where it has been altered during the filtering process in the level 4 step. For example, if the concentration was set to 0 in `ice_conc` due to the open water filter, then the original (raw) value will be available in `raw_ice_conc_values`. This variable is masked (with missing values) outside the maximum sea ice climatology and where the sea ice concentration is unaltered by the filters (in both case the sea-ice concentration value can be accessed from `ice_conc`). This variable can also contain un-physical ice concentration values such as values below 0% and above 100%. **This variable is for use by more advanced users**, who can take advantage of information with less filtering applied, e.g. via Data Assimilation techniques or for validation (Kern et al. 2019). An example can be seen in Figure 7.

`raw_ice_conc_values` must be used together with `ice_conc` to reconstruct the unfiltered field of sea-ice concentration values as in the code example below. This is a bit more work, but ensures that no user accesses full maps of unfiltered sea-ice concentrations (including values below 0% and above 100%) by accident.

```
import xarray as xr

ds = xr.open_dataset(url_or_path_to_a_product_file)

ice_conc = ds['ice_conc'].to_masked_array()
raw_ice_conc_values = ds['raw_ice_conc_values'].to_masked_array()
status_flag = ds['status_flag'].to_masked_array().astype('short')

# combine ice_conc with raw_ice_conc_values using the status_flag
ice_conc[ice_conc==100] = raw_ice_conc_values[ice_conc==100]
ice_conc[(status_flag & 4) == 4] = raw_ice_conc_values[(status_flag & 4) == 4]

# ice_conc now holds the full non-filtered SIC field.
```

Code Example: Reconstructing the full non-filtered SIC field from ice_conc, raw_ice_conc_values, and status_flags.

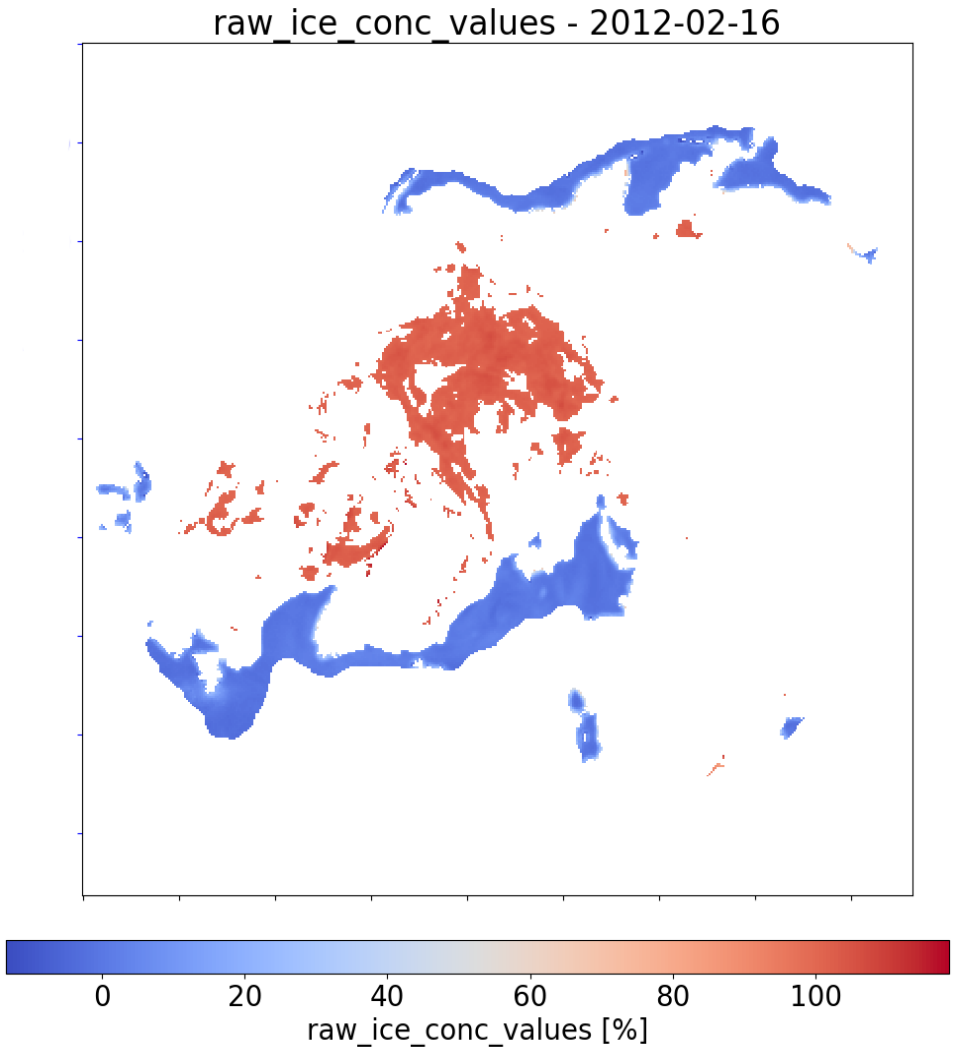

Figure 7: Content of variable `raw_ice_conc_values` from OSI-450-a on 16th February 2012. Missing values appear where `ice_conc` is missing (e.g. over land), outside the maximum ice extent climatology (`ice_conc` set to 0), and where `raw_ice_conc_values` would be the same as those in `ice_conc` (in which case they only appear in `ice_conc`).

Another example of `raw_ice_conc_values` variable is shown in Figure 8. The blue belt is the region where the open water filter was triggered. The corresponding grid cells in variable `ice_conc` will show exactly 0%, removing a lot of the weather-induced noise in this region (values in the range -4%;+4%). Note also how a few pixel wide zone of potentially true, low concentration sea ice (+5%;+15%) is removed by the filter. This is the major drawback of using open water filters (*aka* weather filters) for sea ice concentration filtering: some true ice is removed at the marginal ice zone (see section 6.1.1).

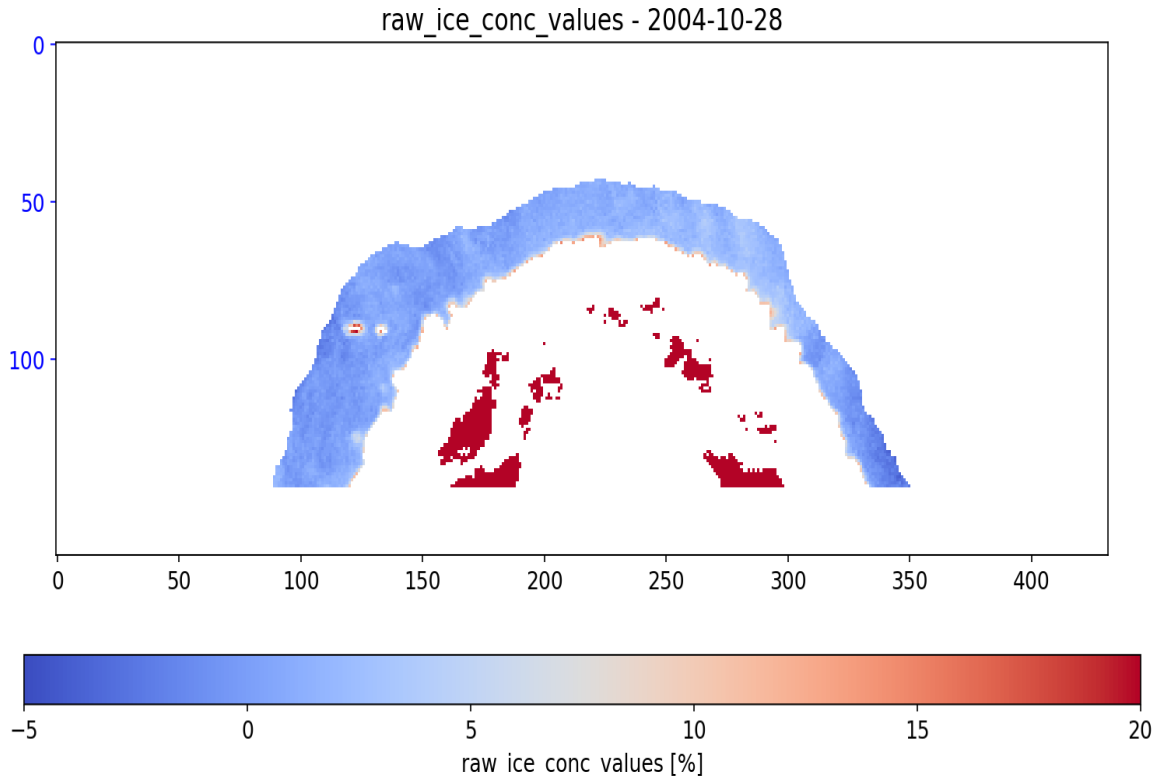

Figure 8: Example of the `raw_ice_conc_values` field on 28th October 2004 in the Southern Hemisphere. The blue belt is where the open water filter was triggered (note the range of the color bar saturates at 20% SIC).

Grid cells around islands and land (e.g. South Georgia, Graham Land) in Figure 8 are not affected by the open water filter, but are present as a result of land spill-over correction.

5.1.3 Uncertainty estimates

An estimate of the uncertainty of the sea ice concentration value in a grid cell is given in the separate standard_uncertainty fields. The uncertainty is given as one standard deviation in percentage. Three maps of uncertainty information are provided in each file, the algorithm standard uncertainty, the smearing standard uncertainty, and the total standard uncertainty. The total uncertainty is the combination (the square root of the sum of variances) of the two other components of the uncertainty budget. An example is shown in Figure 9.

More details about the calculation of the uncertainty can be found in the ATBD [RD-1].

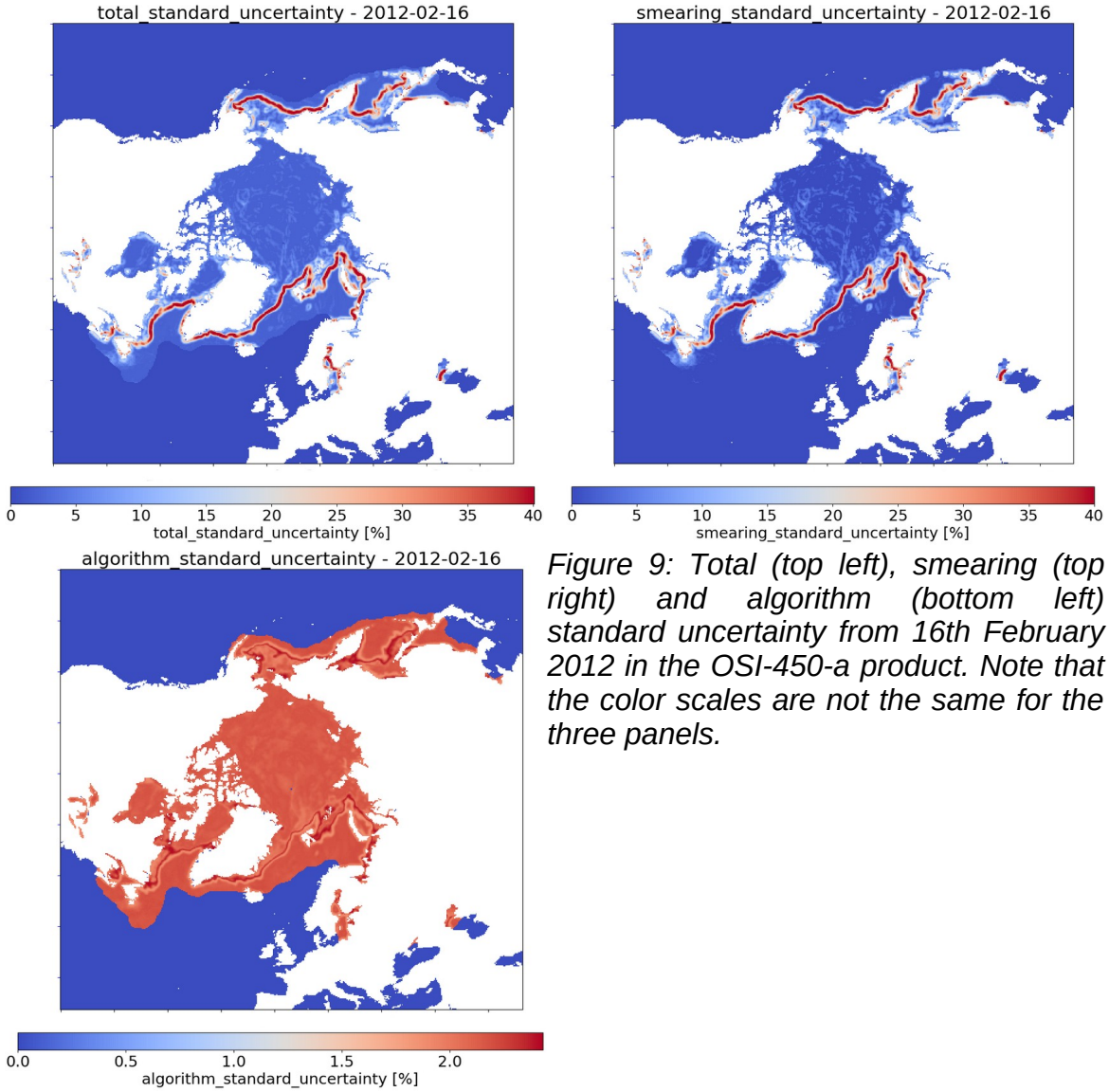

Figure 9: Total (top left), smearing (top right) and algorithm (bottom left) standard uncertainty from 16th February 2012 in the OSI-450-a product. Note that the color scales are not the same for the three panels.

5.1.4 Status flag

The status flag contains information about the processing steps that have influenced the ice concentration value. It is coded as a signed character. The different values are described in Table 4.

Bit Nr	Value	Definition
1	1	Position is over land
2	2	Position is lake
3	4	SIC is set to zero by the open water filter
4	8	SIC value is changed for correcting land spill-over effects
5	16	Handle with caution, the 2m air temperature is high (>=5 degrees Celsius) at this position, and this might be false ice
6	32	Value is the result of spatial interpolation
7	64	Value is the result of temporal interpolation
8	128	SIC is set to zero since position is outside maximum sea ice climatology

Table 4: Definition of sea ice concentration status flag bits.

This value is a bit array with each bit representing a different status, so grid cell values can be a combination of several statuses. One example of this that may occur is an area where the concentration has been gapfilled using spatial interpolation and where the open water filter kicks in setting the concentration to zero. This cell would then have the value 36 (a combination of the spatial interpolation (32) and open water filter (4) values) since the individual flag values are combined.

Most combinations of flags are theoretically possible, with the exception of the eightth (outside maximum climatology) and first (land) bits that both override other flags in the grid cells. Another excluded possibility is a combination of the third (open water filter) and fourth (land spill-over correction) bits, but this is due to their applicable areas not overlapping. Also, the value in a grid cell can't be both spatially and temporally interpolated.

5.1.5 Monthly product files

The description above was mainly focused on the daily product files, which are the main content of the v3 CDRs. Monthly product files are also made available, that simply contain fields of mean SIC for one month. The monthly product files are on the same EASE2 grids as the daily product files and share the same file structure.

A notable difference is that the monthly product files only have the main SIC variable (ice_conc), the secondary SIC variable (raw_ice_conc_values), and processing flags (status_flag). The monthly product file thus do not include uncertainty fields, because this would require knowledge of the spatio-temporal correlation lengths of the daily uncertainty and because the monthly product targets a user community that so far did not express the need for such uncertainty information.

Importantly: monthly-mean SIC values below 10% SIC are cut from the ice_conc variable (where they are assigned a value of 0% SIC) and reported in the raw_ice_conc_values variable instead. This is to be consistent with the daily SIC product files (where the same 10% cut-off is embedded in the open water filters). Users are advise to reconstruct the full SIC field by combining the content of ice_conc and raw_ice_conc_values.

In case of missing days, no temporal interpolation is used in building the monthly product files. If data are missing for more than 5 consecutive days, the monthly product file is not produced. Table 8 lists the months for which no monthly-mean files could be prepared.

5.2 Grid specification

For a given day, northern and southern hemisphere maps of sea ice concentration are available in two separate files. For both hemispheres, the sea ice concentration product is presented on a Lambert Azimuthal Equal Area polar projection, with a grid spacing of 25.0

km. The Lambert grid is also called the EASE2 grid, and is used by NSIDC for several of their sea ice and snow products. More documentation about the EASE2 grid can be found on their web site: http://nsidc.org/data/ease/.

The details of the grid definitions are given in Table 5 and illustrated on Figure 3. Projection definitions in the form of PROJ-4 initialization strings are also given.

Projection:	Lambert Azimuthal Equal Area (EASE2)
Resolution:	25.0 km
Size:	432 columns, 432 rows
Central Meridian:	0°
Datum/Earth:	WGS84 (a=6378137.0 m , b=6356752.314245 m)
PROJ-4 string:	NH: +proj=laea +ellps=WGS84 +datum=WGS84 +lat_0=90 +lon_0=0 SH: +proj=laea +ellps=WGS84 + datum=WGS84 +lat_0=-90 +lon_0=0

Table 5: Geographical definition for the EASE2 25.0 km grid, Northern and Southern Hemisphere.

5.3 Meta data specification

The meta data included in the product file are given as NetCDF attributes to the variables and to the file (Global Attributes). Attributes associated to the variables are those required by the CF convention (http://cfconventions.org/), and all attributes follow the Attribute Convention for Data Discovery (ACDD) v1.3 (http://wiki.esipfed.org/index.php/Attribute_Convention_for_Data_Discovery_(ACDD)). NASA GCMD and IMO keywords were also selected.

5.4 File naming convention

5.4.1 Daily SIC files

The NetCDF/CF product files with daily SIC fields have the following naming convention:

`ice_conc_<area>_ease2-250_<prodID>_<date12>.nc` ,

where:

`<area>` : <nh> (Northern Hemisphere) and <sh> (Southern Hemisphere)

<prodID> : see Table 6.

`<date12>` : central date of the analysis <YYYYMMDD1200>, e.g. 199112021200.

OSI-450-a	OSI-458	OSI-430-a	OSI-430-a (fast-track)
`cdr-v3p0`	`cdr-v3p0-amsr`	`icdr-v3p0`	`icdrft-v3p0`

Table 6: Values of field <prodID> in the filenames for the SIC CDRs

5.4.2 Monthly SIC files

The monthly averaged sea-ice concentration files from OSI-450-a and OSI-430-a (processed monthly) follow a slightly different filename convention:

`ice_conc_<area>_ease2-250_<prodID>_<month>.nc` ,

where:

<area> : <nh> (Northern Hemisphere) and <sh> (Southern Hemisphere)

<prodID> : cdr-v3p0 (for OSI-450-a) and icdr-v3p0 (for OSI-430-a).

<month> : valid month <YYYYMM>, e.g. 199112.

5.5 Product delivery and timeliness

5.5.1 Climate data record OSI-450-a and OSI-458

This OSI SAF sea ice concentration climate data record covers the period from 25.10.1978 to 31.12.2020. Some dates are missing due to lack of satellite data. These dates are listed in Appendix A.

The data set is distributed freely through the OSI SAF Sea Ice FTP server: ftp://osisaf.met.no/reprocessed/ice/conc/v3p0/

The daily data files are organized in YYYY/MM/ sub-directories.

The monthly average data files are organized in YYYY/ sub-directories at this address: ftp://osisaf.met.no/reprocessed/ice/conc/v3p0/monthly/

Note that most web browser no more support the FTP protocol and that you must use dedicated tool such as the ftp command line or FileZilla.

The same data files are serviced through THREDDS, HTTP, OpenDAP, WMS, and netCDF Sub-setter protocols at https://thredds.met.no/thredds/osisaf/osisaf_cdrseaiceconc.html.

Finally, the data set is also available in the EUMETSAT Data Centre. More information about this is available here:

http://www.eumetsat.int/website/home/Data/DataDelivery/EUMETSATDataCentre/index.html

5.5.2 Continuous updates product (ICDR) OSI-430-a

The OSI-430-b ICDR files are available on OSI SAF Sea Ice FTP server: ftp://osisaf.met.no/reprocessed/ice/conc-cont-reproc/v3p0

The daily data files are organized in YYYY/MM directories. Both the “nominal” ICDR files (`icdr-v3p0`) and the most recent 15 days of “fast-track” ICDR files (`icdrft-v3p0`) are available there.

The monthly average data files are in YYYY directories at this address: ftp://osisaf.met.no/reprocessed/ice/conc-cont-reproc/v3p0/monthly/

Note that most web browser no more support the FTP protocol and that you must use dedicated tool such as the ftp command line or FileZilla.

The same data files are serviced through THREDDS, HTTP, OpenDAP, WMS, and netCDF Sub-setter protocols at https://thredds.met.no/thredds/osisaf/osisaf_crepseaiceconc.html.

Finally, the data set is also available in the EUMETSAT Data Centre. More information about this is available here:

http://www.eumetsat.int/website/home/Data/DataDelivery/EUMETSATDataCentre/index.html

5.6 File format differences to the v2 CDRs (OSI-450 and SICCI-25km)

At a technical level, the v3 SIC CDR files are very similar to those of the v2 CDRs. They have the same projection and grid, the same CF structure, the same status flags, etc… The most notable differences are:

- New name for the uncertainty variables: now named "_uncertainty" instead of "_error"
- Updates to some global attributes, especially those describing the source data;
- Updates to the filename format of the CDR based on AMSR (SICCI-25km → OSI-458).

5.7 Complementarity of the v3 SIC CDRs from OSI SAF and ESA CCI+

As mentionned in section 1.4 , the ESA CCI+ Sea Ice project (2019-2022) prepares its own SIC CDRs. At time of writing this PUM, the CCI+ CDRs have not been released nor assessed yet and it is thus not possible to go into great detail in comparing CDRs from the two projects.

The CCI+ Sea Ice project mainly aims at two SIC CDRs:

- A CDR from the Nimbus-5 Electrically Scanning Microwave Radiometer (ESMR) covering the period 1972 – 1975 (with data gaps). Nimbus-5 ESMR was a single-channel cross-track scanning radiometer. New algorithms and radiative transfer models have been developed in the ESA CCI+ Sea Ice project. The data will be highly relevant for users of OSI-450-a that need sea-ice information from the early and mid 1970s. There is no overlap with the OSI SAF v3 CDRs.
- A CDR using the near-90 GHz imagery of the SSM/I and SSMIS missions, covering the period 1991 – 2020. This CCI+ CDR thus uses the same missions as OSI-450-a, but adds the use of the near-90 GHz imagery that has a better spatial resolution. Algorithm development activities in ESA CCI+ concluded that an effective way of using the near-90 GHz imagery was in combination with SICs derived from the 19 and 37 GHz imagery with an pan-sharpening algorithm. In short, this ESA CCI+ SIC CDR will be an enhanced-resolution (12.5 km instead of 25 km) version of OSI-450-a for the period 1991 – 2020 (~30 years). It is limited to 30 years only because the near-90 GHz imagery was only available from the SSM/I F10 mission. This CCI+ SIC CDR should thus be an interesting data source for more regional and shorter applications (including reanalyses). Being primarily an R&D initiative, this CDR will not have an ICDR in the context of CCI+. A validation exercise conducted in CCI+ will allow documenting the improved spatial resolution but also the potentially reduced accuracy coming from using the near-90 GHz imagery (more sensitive to cloud liquid water and surface temperature variations).

Both CCI+ SIC CDRs are expected to be released by late 2022.

6. Known limitations

Known limitations of the reprocessed sea ice concentration products are listed in this section. All the aspects listed apply in large extent to the other existing Sea Ice Concentration datasets based on Passive Microwave Radiometer (PMR) measurements. Users of the OSI SAF and other similar data sets, should be fully aware of these so as not to bias their conclusions.

6.1.1 Removal of true ice by the open water filters

The open water filter (aka weather filter) implemented in our SIC CDRs is based on combination of the PMR channels around 19 GHz and 37 GHz (Gloersen and Cavalieri, 1986). Although the filter is efficient at detecting and removing weather-induced noise over open water, it is also known to remove some amount of true low-concentration ice, especially in the marginal ice zone. The tuning of the open water filter is a trade-off between a) ensuring that no weather induced false ice is found in the maps and b) keeping the low range of true sea ice concentration as close to reality. It is also of prime importance that the open water filter is consistent throughout the time-series and across the changes of sensing frequencies (Kern et al., 2019).

For the OSI-450 v2 CDR, a dynamic tuning of the filter was adopted. The tuning is done in such a way that the filter detects as open water (and thus sets 0% in the `ice_conc` variable) 1) all weather-induced false ice over ocean, and 2) potentially true sea ice up to 10% concentration. This 10% target is however only valid on average atmospheric conditions, and more compact ice might be affected by the filter as well (Andersen et al. 2006B; Ivanova et al. 2015).

See also the discussion in section 5.1.2 .

The effect of the open water filter is not included in the uncertainty variables. The uncertainty variables are pertaining to the un-filtered (raw) ice concentration values. It is noted that the open water filters were slightly revised for the v3 CDRs (see ATBD [RD-1]).

6.1.2 Summer melt and melt-ponding

Virtually all SIC algorithms based on the PMR channels around 19GHz, 37GHz, and 90GHz are very sensitive to surface melt and melt-pond water on top of the ice. In the early phase of melt, wet and warm snow has a higher emissivity than during winter (Kern et al., 2016). This change of emissivity before ponding is well captured by the dynamic tie-point approach implemented in our CDRs (Kern et al. 2020).

When melt-ponds appear on top of the ice, the radiation emitted at the microwave wavelengths used in SIC algorithms comes from a very thin water layer, which does not allow for distinguishing between ocean water (in leads) and melt water (in ponds). Based on these principles, the `ice_conc` variable of PMR SIC products should thus hold an estimate of 1 minus the open water fraction in each grid cell, irrespective if this water is from ocean or ponds (the net surface water fraction). However, Kern et al. (2020) recently showed that no existing PMR SIC data records performed satisfactorily during the melt season, neither in terms of true SIC, nor in terms of net surface water fraction.

The uncertainty variables in the OSI SAF SIC CDRs are larger during the summer melt seasons, even though the misinterpretation of meltwater as open water is not explicitly included in the uncertainty propagation. We have no reasons to believe that the v3 CDRs will behave better than the v2 CDRs during the summer melt season, this requires more research.

6.1.3 Thin and bare sea ice

Concentration of thin sea ice (< 30cm) is underestimated by most of the “classic” PMR SIC algorithms, due to the radiometric contribution of water below the ice. A complete, 100% cover of thin sea-ice, especially if it is predominantly bare, indeed does not act as a radiometric insulator for the PMR frequencies around 19 and 37 GHz that are the base for this OSI SAF dataset, and many others. This is for example discussed in Ivanova et al. (2015).

The mis-interpretation of thin 100% sea ice coverage as ice with a lower concentration is not included in the uncertainty variables. We have no reasons to believe that the v3 CDRs will behave better than the v2 CDRs for thin sea ice conditions, this requires more research.

6.1.4 Interpolation of missing values

The OSI SAF SIC dataset aims at addressing needs from all users needing access to climate sea ice concentration data, from interested general public to climate modelers. It was decided to provide interpolated sea ice concentration values in places where original input satellite data was missing, aiming at most complete daily maps. Both temporal and spatial interpolation is used. The locations where interpolation was used are clearly identified in the status_flag layer (see 5.1.4).

These interpolated sea ice concentration values should generally be used with caution for scientific applications, especially the values obtained from spatial interpolation. The uncertainty variables are not interpolated where data was missing.

The methodology for spatial interpolation was largely revised for the v3 SIC CDRs (and specifically OSI-450-a) by adopting the algorithm of Strong and Golden (2016).

6.1.5 Grid resolutions

The OSI-450-a and OSI-430-a SIC fields are presented at 25km grid spacing. However, a spatial sampling of 25 km does not fully represent the true spatial resolution of the product. Indeed, the footprint of the SSM/I channels used in the product is 43x69km at the 19GHz channel and 28x37km at the 37GHz channel. Thus, the true resolution is coarser than the spatial sampling of the product grid.

This is not the case for the OSI-458 SIC fields. These are presented at 25 km grid spacing, but since the AMSR-E and AMSR2 imagery have footprints close to or better than 25 km, the true resolution should be well represented by the product grid. See Figure 6.

6.1.6 Coastal regions

The radiometric signature of land is similar to sea ice at the wavelengths used for estimating the SIC. Because of the large foot-prints and the relatively high brightness temperatures of land and ice compared to water, the land signature is “spilling” into the coastal zone open water and it will falsely look as intermediate concentration ice. Thanks to the better resolution of the imagery of AMSR missions, there is less land-spillover for OSI-458 and for OSI-450-a and OSI-430-a.

The land-spill-over effect is corrected for as described in the ATBD [RD-1]. However, this coastal correction procedure is not perfect, and a level of false sea-ice remains along some coastlines. The uncertainty variables have larger values in the coastal regions where land spill-over effects are detected.

The land spill-over correction scheme was improved for the v3 SIC CDR (see ATBD [RD-1]) and the validation exercise confirmed that there are less land spill-over effects in v3 than in v2 (see VALR [RD-2]).

6.1.7 Lake ice

The retrieval of fresh water lake ice concentration is challenging when using coarse resolution microwave imagery. First, ice concentration retrievals suffer from land spill-over effects (section 6.1.6). Second, the microwave emissivity of lake ice is different from that of sea ice and would require specific algorithm tie-points. In the v3 SIC CDRs we removed many small and medium lakes with our land mask (Figure 3) to reduce the issue but still call for caution when using the ice concentration values over lakes (as identified in the status_flag, section 5.1.4).

The Great Lakes are one of the lake systems where we provide ice concentration values. We call for extra caution at the start of the OSI-450-a time-series due to the use of ERA5 data: An issue with ERA5 2m temperatures over the Great Lakes (especially Lake Superior) results in a cold bias in Jan-May and a warm bias in Jun-Dec during 1979-2013 (Simmons et al, 2021).

7. References

Andersen, S., L. Toudal Pedersen, G. Heygster, R. Tonboe, and L Kaleschke, Intercomparison of passive microwave sea ice concentration retrievals over the high concentration Arctic sea ice. *Journal of Geophysical Research* 112, C08004, doi10.1029/2006JC003543, 2007.

Andersen, S., R. Tonboe, S. Kern, and H. Schyberg. Improved retrieval of sea ice total concentration from spaceborne passive microwave observations using Numerical Weather Prediction model fields: An intercomparison of nine algorithms. *Remote Sensing of Environment104, 374-392*, 2006B.

Ashcroft, P. and Wentz, F. J.: AMSR-E/Aqua L2A Global Swath Spatially-Resampled Brightness Temperatures, Version 3 [2002–2010], NASA National Snow and Ice Data Center Distributed Active Archive Center, Boulder, Colorado, USA, https://doi.org/10.5067/AMSR-E/AE_L2A.003, 2013.

Fennig, K., Schröder, M., Andersson, A., and Hollmann, R.: A Fundamental Climate Data Record of SMMR, SSM/I, and SSMIS brightness temperatures, Earth Syst. Sci. Data, 12, 647–681, https://doi.org/10.5194/essd-12-647-2020, 2020.

Gloersen, P., and F. T. Barath. A scanning multichannel microwave radiometer for Nimbus-G and SeaSat-A. *IEEE Journal of Oceanic Engineering OE-2*(2), 172-178, 1977.

Gloersen, P., and D. J. Cavalieri (1986), Reduction of weather effects in the calculation of sea ice concentration from microwave radiances, J. Geophys. Res., 91(C3), 3913–3919, doi:10.1029/JC091iC03p03913.

Gloersen, P., W. J. Campbell, D. J. Cavalieri, J. C. Comiso, C. L. Parkinson, H. J. Zwally. Arctic and Antarctic sea ice, 1978-1987: satellite passive-microwave observations and analysis. *NASA SP-511*, Washington D. C., 1992.

Ivanova, N., Pedersen, L. T., Tonboe, R. T., Kern, S., Heygster, G., Lavergne, T., Sørensen, A., Saldo, R., Dybkjær, G., Brucker, L., and Shokr, M.: Inter-comparison and evaluation of sea ice algorithms: towards further identification of challenges and optimal approach using passive microwave observations, The Cryosphere, 9, 1797-1817, doi:10.5194/tc-9-1797-2015, 2015.

Kern, S., Rösel, A., Pedersen, L. T., Ivanova, N., Saldo, R., and Tonboe, R. T.: The impact of melt ponds on summertime microwave brightness temperatures and sea-ice concentrations, The Cryosphere, 10, 2217-2239, doi:10.5194/tc-10-2217-2016, 2016.

Kern, S., Lavergne, T., Notz, D., Pedersen, L. T., Tonboe, R. T., Saldo, R., and Sørensen, A. M.: Satellite passive microwave sea-ice concentration data set intercomparison: closed ice and ship-based observations, The Cryosphere, 13, 3261–3307, https://doi.org/10.5194/tc-13-3261-2019, 2019.

Kern, S., Lavergne, T., Notz, D., Pedersen, L. T., and Tonboe, R.: Satellite passive microwave sea-ice concentration data set inter-comparison for Arctic summer conditions, The Cryosphere, 14, 2469–2493, https://doi.org/10.5194/tc-14-2469-2020, 2020.

Lavergne, T., Sørensen, A. M., Kern, S., Tonboe, R., Notz, D., Aaboe, S., Bell, L., Dybkjær, G., Eastwood, S., Gabarro, C., Heygster, G., Killie, M. A., Brandt Kreiner, M., Lavelle, J., Saldo, R., Sandven, S., and Pedersen, L. T.: Version 2 of the EUMETSAT OSI SAF and ESA CCI sea-ice concentration climate data records, The Cryosphere, 13, 49-78, https://doi.org/10.5194/tc-13-49-2019, 2019.

Meier, W., Fetterer, F., Savoie, M., Mallory, S., Duerr, R., and Stroeve, J.: NOAA/NSIDC Climate Data Record of Passive Microwave Sea Ice Concentration, Version 3, NSIDC: National Snow and Ice Data Center, Boulder, Colorado, USA, https://doi.org/10.7265/N59P2ZTG, 2017.

Parkinson C.L. A 40-y record reveals gradual Antarctic sea ice increases followed by decreases at rates far exceeding the rates seen in the Arctic, PNAS, 116 (29) (2019), pp. 14414-14423, 2019.

Peng, G., Meier, W. N., Scott, D. J., and Savoie, M. H.: A long-term and reproducible passive microwave sea ice concentration data record for climate studies and monitoring, Earth Syst. Sci. Data, 5, 311–318, https://doi.org/10.5194/essd-5-311-2013, 2013.

Simmons, A., Hersbach, H., Munoz-Sabater, J., Nicolas, J., Vamborg, F., Berrisford, P., de Rosnay, P., Willett, K. and Woollen, J.: Low frequency variability and trends in surface air temperature and humidity from ERA5 and other datasets. ECMWF Technical Memorandum 881, https://doi.org/10.21957/ly5vbtbfd, 2021.

Strong, C. and Golden, K. M.: Filling the Polar Data Gap in Sea Ice Concentration Fields Using Partial Differential Equations, Remote Sens., 8, 442, https://doi.org/10.3390/rs8060442, 2016.

Tonboe, R. T., Eastwood, S., Lavergne, T., Sørensen, A. M., Rathmann, N., Dybkjær, G., Pedersen, L. T., Høyer, J. L., and Kern, S.: The EUMETSAT sea ice concentration climate data record, The Cryosphere, 10, 2275-2290, doi:10.5194/tc-10-2275-2016, 2016.

Wentz, F. J. A model function for ocean microwave brightness temperatures. *Journal of Geophysical Research 88*(C3), 1892-1908, 1983.

Wentz, F. J. A well-calibrated ocean algorithm for SSM/I. *Journal of Geophysical Research* 102(C4), 8703-8718, 1997.

Wentz, F. J. User's Manual, SSM/I Antenna Temperature, Version 6. *RSS Technical Memo 082806*, 2006.

8. Appendix A: Missing dates

The v3 CDRs cover the period from 25.10.1978 to 31.12.2020. During the SMMR period only every second day is available. Table 7 below lists the dates with no daily product files due to lack of satellite data, except the expected missing SMMR days (every second day). The SMMR data is used until 20.08.1987. Table 8 lists the months for which the monthly product files are missing.

Year	***Missing daily CDR files***
SMMR	
1978	
1979	21/5-27/5
1980	4/1-10/1, 27/2-4/3, 16/3-22/3, 9/4-15/4
1981	27/2-5/3
1982	14/7-16/7, 30/7-1/8, 3/8-5/8, 15/8-17/8
1984	12/8-24/8
1985	22/9-28/9
1986	29/3-23/6, 8/12-10/12, 16/12-18/12
1987	3/1-15/1, 7/4-9/4
SSM/I	
1987	25/08-26/08, 06/10-07/10, 03/12-31/12
1988	01/01-12/01, 06/05-09/05, 23/09, 25/12-27/12
1989	14/01, 07/06, 21-22/07 (SH), 23/07-24/07, 23/10
1990	13/08, 25/08-26/08, 21/10-22/10, 26/10-28/10, 21/12 (NH), 22/12-26/12
2000	01/12
SSMIS	
2021	20/02
2022	09/11
AMSR-E	
	None
AMSR2	
	None

Table 7: Dates with missing daily CDR product files due to lack of satellite data. SMMR (25.10.1978-20.08.1987) was operated every second day and the table shows only the periods with missing SMMR data for more than one day.

Year	***Missing monthly SIC files***
SMMR	
1978	October
1986	April, May, June
SSM/I	
1987	December
SSMIS	
	None

Table 8: Dates with missing monthly CDR product files due to lack of satellite data.